

Effect of excitability on partially pinned scroll waves in excitable chemical mediaKritsana Khaothong ¹, Jarin Osaklung,¹ Malee Sutthiopad,¹ Jiraporn Luengviriyaya,²
Kenneth Showalter ³ and Chaiya Luengviriyaya^{1,*}¹*Department of Physics, Kasetsart University, 50 Phaholyothin Road, Jatujak, Bangkok 10900, Thailand*²*Lasers and Optics Research Center, Department of Industrial Physics and Medical Instrumentation, King Mongkut's University of
Technology North Bangkok, 1518 Pibulsongkram Road, Bangkok 10800, Thailand*³*C. Eugene Bennett Department of Chemistry, West Virginia University, Morgantown, West Virginia 26506-6045, USA*

(Received 5 June 2023; accepted 13 October 2023; published 1 November 2023)

We present an investigation of excitability effects on the dynamics of scroll waves partially pinned to inert cylindrical obstacles in three-dimensional Belousov-Zhabotinsky excitable media. We also report on corresponding numerical simulations with the Oregonator model. The excitability varies according to the concentration of sulfuric acid $[H_2SO_4]$ in the Belousov-Zhabotinsky (BZ) reaction and the parameter ε^{-1} in the Oregonator model. Initially, the freely rotating scroll segment rotates faster than the pinned one. The difference in the frequency of the two parts results in a transition from a straight pinned scroll wave to a twisted one, which helically wraps around the entire obstacle. The wave frequency in the whole volume is equal to that of the freely rotating scroll wave. When the excitability is increased, the time for the transition to the twisted wave structure decreases while the average speed s of the development increases. After the transition, the twisted wave remains stable. In media with higher excitability, the helical pitch is shorter but the twist rate ω is higher. Analysis presented in this study together with our previous findings of the effect of the cylindrical obstacle diameter on the wave dynamics results in common features: The average speed s and the twist rate ω of both studies fit well to functions of the difference in the initial frequency Δf of the freely rotating and untwisted pinned waves. We also demonstrate the robustness of the partially pinned scroll waves against perturbations from spontaneous waves emerging during the wave generation in the BZ medium with high $[H_2SO_4]$. Even though the scroll wave is partly disturbed at the beginning of the experiment, the spontaneous waves are gradually suppressed and the typical wave structure is finally developed.

DOI: [10.1103/PhysRevE.108.054201](https://doi.org/10.1103/PhysRevE.108.054201)**I. INTRODUCTION**

Thin layers of excitable media have been found to support self-organizing patterns such as spiral waves [1–5]. For thicker media, three-dimensional (3D) versions of spiral waves, namely, scroll waves [6], have more complicated dynamics due to the third dimension. The scroll waves rotate around lines of phase singularities called filaments, which can be simple straight lines, closed loops, or complicated structures [7].

Scroll waves are crucial to human health because they are involved in cardiac arrhythmia such as atrial and ventricular tachycardia. Moreover, when the scroll waves become unstable and then are broken into multiple uncoordinated segments, i.e., electrical turbulence, a life-threatening cardiac fibrillation may occur [8,9]. The wave breakups have been found to arise from different mechanisms [10]. They can originate even from simple straight scroll waves in homogeneous media with excitability in regimes known as the negative tension instability [11–15] and the three-dimensional (3D) meandering instability [12,15–17].

A gradient of excitability can generate scroll wave instability. A straight scroll wave becomes a twisted wave after being

subjected to a gradient along its filament. A twist-induced instability occurs when the twisted filament deforms into a helical one [18,19,12]. The twist-induced instability has been demonstrated in the Belousov-Zhabotinsky (BZ) reaction with a gradient of temperature [20,21], oxygen [22] or CO_2 concentration [23,24].

It has been discovered that veins or scars potentially act as obstacles that pin electrical spiral waves in cardiac tissues and may cause the corresponding tachycardia to stay longer [25]. The pinned spiral waves propagate with period, wavelength, and speed increased by the obstacle circumference [26–30]. Furthermore, the increasing of the wave speed by the obstacle enhances the difficulty of the elimination of the pinned spiral waves by using a wave train [31,32] or external forcing [33,34].

In 3D systems, the influence of obstacles on the dynamics of scroll waves has been investigated in various situations. A partial pinning causes scroll rings, whose filaments are closed loops, to survive longer [35,36]. Scroll ring filaments that wrap themselves around cylindrical obstacles are reshaped and the length of the pinned parts increases with time [37]. Repositioning of the pinned waves is demonstrated by using translating cylindrical obstacles. Their filaments are stretched out along the trajectory of the obstacles [38]. A large obstacle which partially pins a scroll wave causes sudden changes in the front velocity at the obstacle boundary and induces a wave

*fscicyl@ku.ac.th

breakup, eventually giving rise to spatiotemporal chaos [39]. In contrast, thin cylindrical obstacles can both suppress the development of spatiotemporal chaos [40] and remove already existing chaotic patterns [40–42].

Recently, we presented a development of helical structures from simple straight scroll waves partially pinned to cylindrical obstacles. While the free parts remain unchanged, the pinned parts become twisted waves whose structures depend on the obstacle diameter, with the larger the diameter, the shorter the helical pitch but the higher the twist rate [43]. In this paper, we investigate the influence of the excitability of media on the dynamics of scroll waves partially pinned to cylindrical obstacles both in experiments with BZ media and in numerical simulations using the Oregonator model [44,45]. Furthermore, we propose a generalization of the findings presented here and our previous study [43].

II. EXPERIMENTS

A. Experimental methods

In this article, the BZ reaction is composed of NaBrO_3 , malonic acid (MA), H_2SO_4 , and ferroin, all purchased from Merck. In addition, the surfactant sodium dodecyl sulfate (SDS, from Fluka) and 1.0% wt/wt agarose gel (from Sigma) are added in the solution to reduce production of CO_2 bubbles and prevent hydrodynamic perturbations, respectively. The gelled BZ medium is prepared as described in [46]. Stock solutions of NaBrO_3 (1 M), MA (1 M), and SDS (1 M) are freshly prepared by dissolving powder in de-ionized water (conductivity of $\sim 0.056 \mu\text{S cm}^{-1}$), whereas stock solutions of H_2SO_4 (2.5 M) and ferroin (25 mM) are commercially available. Appropriate volumes of the stock solutions are mixed and diluted in de-ionized water to form BZ solutions with the following initial concentrations: $[\text{NaBrO}_3] = 50 \text{ mM}$, $[\text{MA}] = 50 \text{ mM}$, $[\text{ferroin}] = 0.625 \text{ mM}$, and $[\text{SDS}] = 0.05 \text{ mM}$, where $[\text{H}_2\text{SO}_4]$ is varied between 100 and 200 mM.

The dynamics of partially pinned scroll waves is studied using a transparent Plexiglas reactor with a volume of $30 \times 40 \times 10 \text{ mm}^3$. As shown in Fig. 1, the reactor is placed between a projector and a color CCD camera (Super-HAD, Sony) to record top projection images with a resolution of $27 \mu\text{m pixel}^{-1}$. During the experiments, the temperature of the laboratory is controlled at $24.0^\circ\text{C} \pm 1.0^\circ\text{C}$ by an air conditioner.

A partially pinned scroll wave is created by using a two-layer method, as described in Refs. [33,43]. A volume of BZ solution ($\sim 30^\circ\text{C}$) is poured into the reactor to form the first layer (5 mm in thickness). During the gelation ($\sim 26^\circ\text{C}$), a plastic cylinder (20.0 mm in length and 2.0 mm in diameter) is placed into the top part of the first layer as the obstacle. A pair of opposite propagating linear wave fronts (30.0 mm in length) is started by the temporary immersion of a silver wire between the obstacle and the edge of the reactor. Another volume of BZ solution ($\sim 30^\circ\text{C}$) is added to the reactor as the second layer when one wave front reaches the obstacle, and the other is eliminated at the boundary of the reactor. The front at the obstacle starts to curl in to form a partially pinned scroll wave.

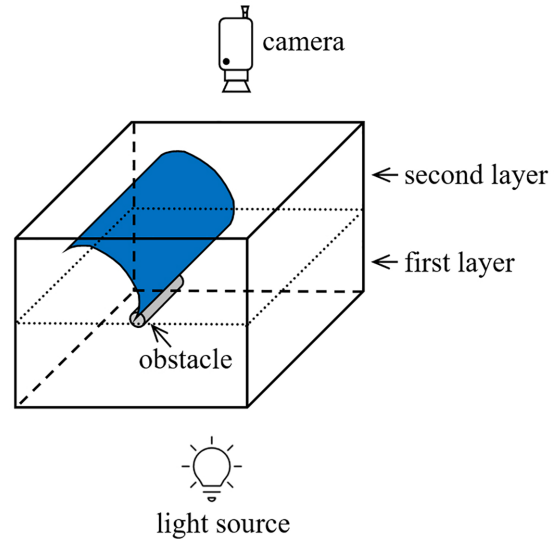


FIG. 1. Sketch of the experimental setup. A two-layer method is used to initiate a scroll wave partially pinned to an obstacle. The reactor is placed between a white light source and a camera to record the top projection of the scroll wave.

B. Experimental results

The evolution of partially pinned scroll waves in this study is similar to that demonstrated recently in [43]. Initially, a straight untwisted scroll wave has two parts: The upper segment rotates freely while the lower segment is pinned to the cylindrical obstacle. During a transient time interval τ , the freely rotating wave rotates faster than the pinned part, so the freely rotating wave advances to displace the slower pinned wave. A twisted wave structure is gradually developed until the whole obstacle is wrapped by the helical wave. Finally, each partially pinned scroll wave consists of the free straight segment and the twisted pinned wave, both rotating with the same period. Examples of images during the development of the twisted scroll wave structure have been illustrated in [43].

Figure 2 reveals the structures of partially pinned scroll waves after a transient time interval in the BZ media with different $[\text{H}_2\text{SO}_4]$. For each scroll wave in Fig. 2, the upper part with 10.0 mm in length is freely rotating, while the lower part is pinned to a cylindrical obstacle of 2.0 mm in diameter and 20.0 mm in length. From the edge of the wave front above the obstacle, we estimate the filament of the freely rotating part using the edge of the wave front above the obstacle, e.g., the dotted line in Fig. 2(a). It is approximately linear at all times during the experiments. In addition, after the transient time interval, the scroll wave structure remains unchanged. Note that for more complicated wave structures, a 3D reconstruction of the scroll waves as well as their filaments may be necessary for analysis, which can be performed with a more complicated observation technique, e.g., optical tomography, as shown in [14,15,17].

From Figs. 2(a)–2(f), it can be clearly seen that the pitch p (i.e., the distance along the obstacle between two points on a helical wave front after one complete turn) decreases when the $[\text{H}_2\text{SO}_4]$ is increased, with a step of 20 mM from 100 to 200 mM. Note that the helical structures develop slowly in these

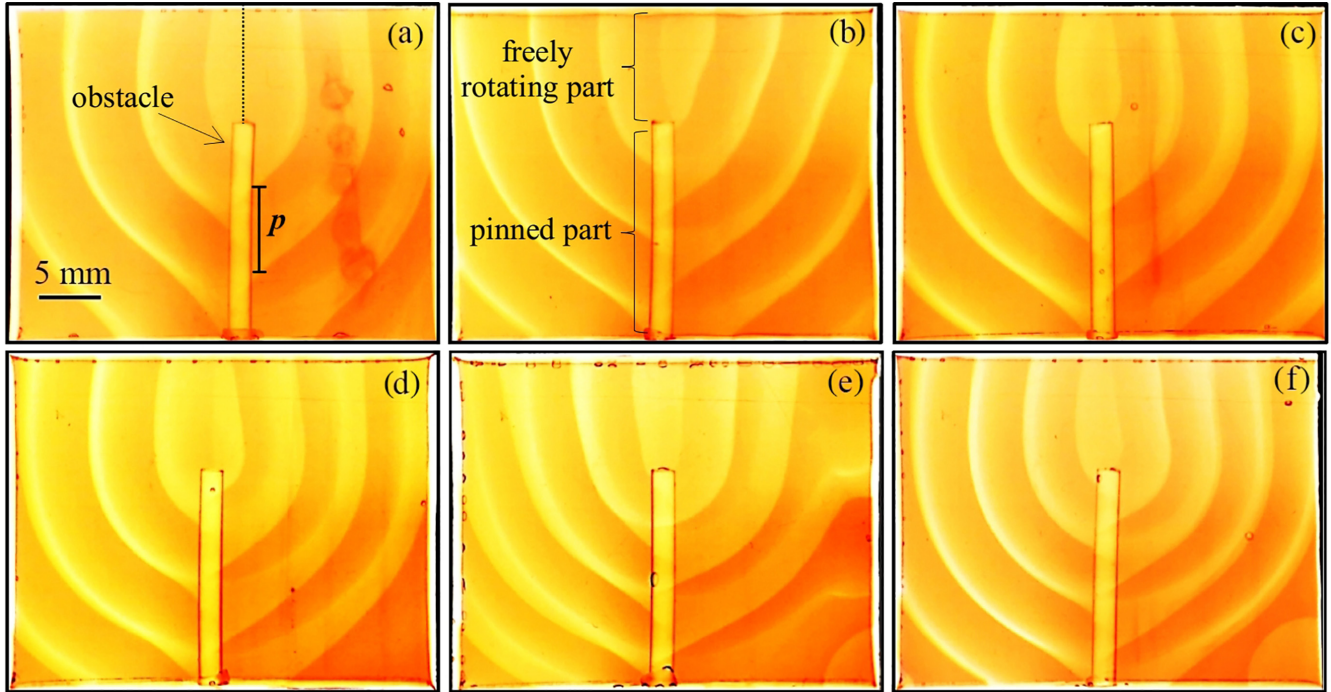


FIG. 2. Projection images of partially pinned scroll waves in excitable BZ media with varying $[\text{H}_2\text{SO}_4]$: (a) 100 mM, (b) 120 mM, (c) 140 mM, (d) 160 mM, (e) 180 mM, and (f) 200 mM. A cylindrical obstacle of 2.0 mm in diameter and 20.0 mm in length is located at the lower center of the images. In (a), the helical pitch p is depicted and the dotted line indicates an estimate of the filament location of the freely rotating wave.

experiments. Figures 2(a)–2(f) show the images at about 256, 157, 120, 95, 81, and 68 min, respectively.

We analyze the dynamics of partially pinned scroll waves with different $[\text{H}_2\text{SO}_4]$, as shown in Fig. 3. All four variables fit as exponential functions of $[\text{H}_2\text{SO}_4]$. When the $[\text{H}_2\text{SO}_4]$ is increased, the transient time interval

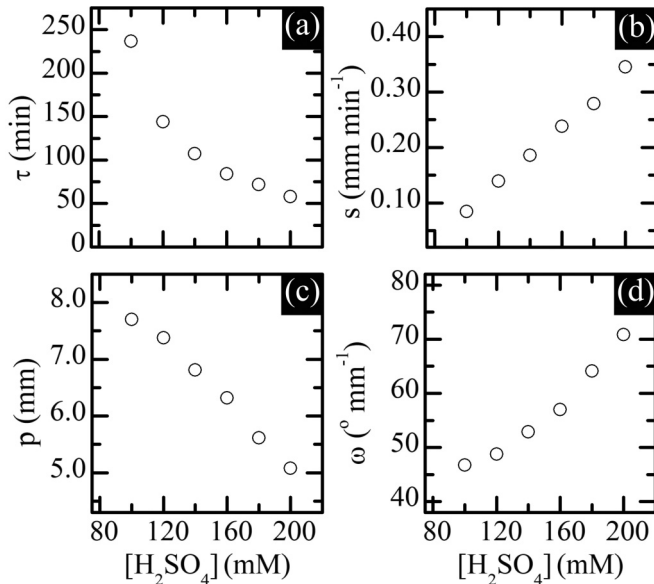


FIG. 3. Analysis of partially pinned scroll waves in BZ media with different values of $[\text{H}_2\text{SO}_4]$: (a) the transient time interval τ , (b) the average speed s , (c) the helical pitch p , and (d) the twist rate ω as functions of $[\text{H}_2\text{SO}_4]$.

τ decreases, with $\tau = 55.99 + 4.76 \times 10^3 \exp(-3.2 \times 10^{-2} [\text{H}_2\text{SO}_4])$ min [Fig. 3(a)], but the twisted structure moves down the obstacle with a higher average speed s ($s = h / \tau$ where h is the obstacle length) $s = -1.89 + 1.75 \exp(1.21 \times 10^{-3} [\text{H}_2\text{SO}_4])$ mm min $^{-1}$ [Fig. 3(b)]. In media with higher $[\text{H}_2\text{SO}_4]$, the structures of scroll waves (which remain unchanged) have shorter helical pitch p , with $p = 11.88 - 2.50 \exp(5.03 \times 10^{-3} [\text{H}_2\text{SO}_4])$ mm [Fig. 3(c)], but higher twist rate ($\omega = 360^\circ / p$), with $\omega = 36.89 + 2.64 \exp(1.28 \times 10^{-3} [\text{H}_2\text{SO}_4])^\circ$ mm $^{-1}$ [Fig. 3(d)].

Changes of the dynamics of the partially pinned scroll waves similar to those in Fig. 3 have been recently illustrated in Ref. [43] in which experiments were carried out with a variation of the obstacle diameter d while $[\text{H}_2\text{SO}_4]$ was kept constant. Even though the experiments in [43] and this study have different conditions, the twisted waves in both studies have the same origin, which is a difference in the initial periods of the pinned part T_{pin} and the free part T_{free} . To compare the current study and our earlier study [43], we measure the initial periods T_{pin} and T_{free} of both studies. An increasing of the obstacle diameter d in our earlier study [43] causes a reduction of T_{pin} but T_{free} is relatively unchanged [Fig. 4(a)], while in the current study, T_{pin} and T_{free} simultaneously decrease when the excitability is increased via $[\text{H}_2\text{SO}_4]$ [Fig. 4(b)].

We now consider the average speed s of the downward motion of the twisted structure and the twist rate ω from both studies. In Fig. 4(c), we plot the average speed s with the difference in the initial frequency Δf which is calculated from T_{pin} and T_{free} in Figs. 4(a) and 4(b), i.e., $\Delta f = f_{\text{free}} - f_{\text{pin}} = (T_{\text{free}})^{-1} - (T_{\text{pin}})^{-1}$, where f_{free} and f_{pin} are the initial frequencies of the free and pinned scroll waves. Even though

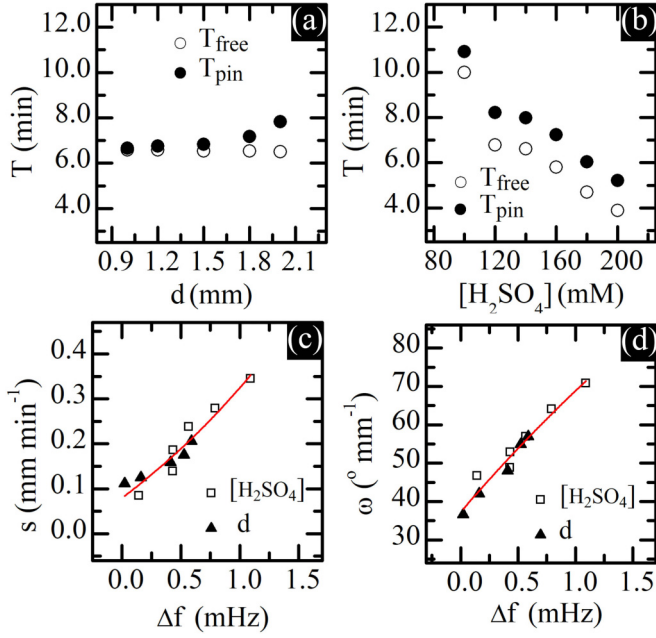


FIG. 4. Common features of partially pinned scroll waves in BZ media. Periods of free and pinned regions at the beginning of experiments, with variations of (a) obstacle diameter d (from Ref. [43]) and (b) $[\text{H}_2\text{SO}_4]$. (c) The average speed s and (d) the twist rate ω of both experimental series, where the diameter d or $[\text{H}_2\text{SO}_4]$ is varied, fit well to exponential functions of the difference in the initial frequency Δf of the free and pinned parts.

changes of the average speed s result from different experimental conditions, with a variation of obstacle diameter d and $[\text{H}_2\text{SO}_4]$ [triangles and squares in Fig. 4(c), respectively], it increases with Δf and is fit with the same exponential function: $s = -0.38 + 0.46\exp(0.42\Delta f)$ mm min^{-1} . Similarly, Fig. 4(d) shows a plot of the twist rate ω from both studies and the data fit with the same exponential function: $\omega = (2.13 \times 10^2) - (1.75 \times 10^2)\exp(-0.19\Delta f)$ $^\circ \text{mm}^{-1}$. The relations in Figs. 4(c) and 4(d) reveal common features of these two different studies and suggest that the difference in the initial frequency Δf is an appropriate variable to describe the dynamics of the partially pinned scroll waves.

It is worth noting that the partially pinned scroll waves are robust against perturbations from spontaneous waves. In BZ media, many spontaneous waves may emerge during the wave initiation and still exist during the development of twisted structures, especially for high $[\text{H}_2\text{SO}_4]$. An example of such situations is shown in Fig. 5. Shortly after the wave initiation is completed, many spontaneous waves occur. In the first few rotations, the upper freely rotating straight waves are clearly seen while most of the lower pinned segment is interrupted and disappears from the projection [Fig. 5(a)]. Most of the spontaneous waves emerge from small points (the black dots in Fig. 5) and then they expand and appear as circular waves in the projection images. In the course of time, the pinned twisted scroll wave gradually develops downward on the obstacle and the spontaneous waves are simultaneously eliminated [Figs. 5(b) and 5(c)]. In this example, the wave twist development is completed within approximately 75 min. Finally, the entire medium is occupied by the partially

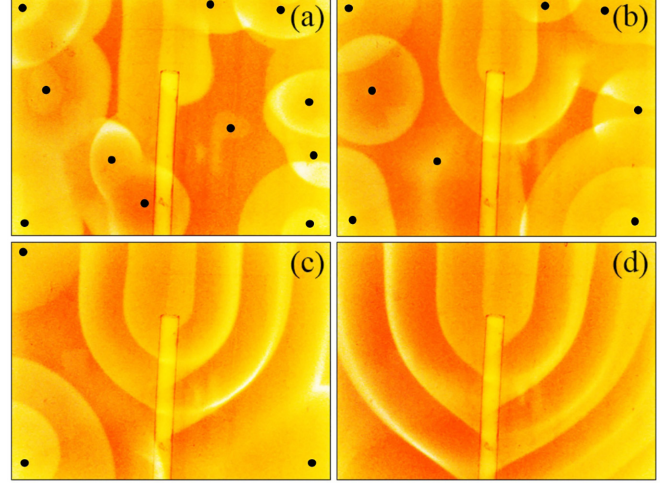


FIG. 5. Suppression of spontaneous waves by a partially pinned scroll wave in the BZ medium with $[\text{H}_2\text{SO}_4] = 180$ mM. Projection images at (a) 10 min: second rotation, (b) 30 min: seventh rotation, (c) 60 min: 14th rotation, and (d) 120 min: 28th rotation. The black dots depict estimates of the centers of spontaneous waves.

pinned scroll wave (in the absence of the spontaneous waves) [Fig. 5(d)].

III. SIMULATIONS

A. Simulation methods

To corroborate the experimental results, we have performed simulations of partially pinned scroll waves using the two-variable Oregonator model [44,45], which describes the reaction-diffusion dynamics of the activator u and the controller v that correspond to the concentrations of the autocatalyst HBrO_2 and the oxidized form of the metal catalyst, respectively, in the BZ reaction:

$$\begin{aligned} \frac{\partial u}{\partial t} &= \frac{1}{\varepsilon} \left(u - u^2 - f v \frac{u-q}{u+q} \right) + D_u \nabla^2 u, \\ \frac{\partial v}{\partial t} &= u - v + D_v \nabla^2 v. \end{aligned} \quad (1)$$

The parameters in Eq. (1) are $q = 0.002$, $f = 1.4$, and the diffusion coefficients $D_u = 1.0$ and $D_v = 0.6$ as in Ref. [45], while the excitability is modulated by parameter $\varepsilon^{-1} = 10 - 200$. We approximate the 3D Laplacian operator by using a 27-point discretization as in [47]. The system size is $60 \times 60 \times 80$ dimensionless space units (s.u.), with a 0.2 s.u. uniform grid space. The time step is set to 0.012 dimensionless time units (t.u.), as required for numerical stability, $\Delta t \leq (3/8)(\Delta x)^2$ [47]. As in Ref. [43], a free scroll wave is initiated by a partition method and allowed to rotate until its shape remains unchanged before a cylindrical obstacle with 4.0 s.u. in diameter and 40.0 s.u. in length is inserted at the core of the wave to form a partially pinned scroll wave. No-flux boundary conditions for the boundaries of the system and for the cylindrical obstacle are applied using the method as described in [48].

B. Simulation results

Even though the generation of the pinned wave in the simulations, where the obstacle is inserted into the preexisting

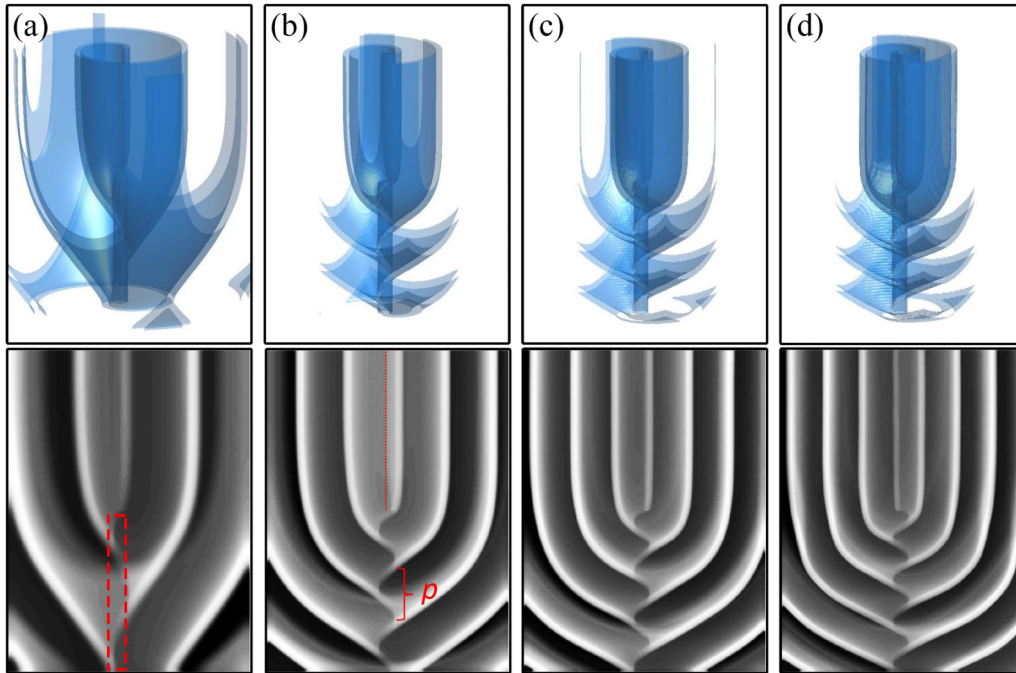


FIG. 6. Images of partially pinned scroll waves in simulations with different excitabilities ε^{-1} : (a) 10, (b) 50, (c) 100, and (d) 200. The top and bottom rows depict isoconcentration surface plots and lateral projections of the volume, respectively. The red dashed rectangle in (a) depicts the position of the cylindrical obstacle. In (b), the helical pitch p is shown and the dotted straight line indicates an estimate of the filament location of the freely rotating wave.

scroll wave, differs slightly from that in the experiments, the development as well as the final structure of the partially pinned scroll wave in both cases are very similar. Figure 6 illustrates examples of partially pinned scroll waves in the simulations with different excitabilities ε^{-1} . In the bottom row, gray-scale images show lateral projections of the activator u in the whole volume. In the top row, the isoconcentration surfaces ($u = 0.4$) are plotted in light blue with a clear background. The outer surfaces in Figs. 6(b)–6(d) are cut out for enhanced visualization of the twisted wave structures near the obstacle.

The partially pinned scroll waves for different excitability ε^{-1} values in Fig. 6 have a very similar structure. The freely rotating part in the upper region of the images is simply a straight scroll wave with a linear filament, while the twisted part in the lower region has a more complicated form of a helical wave which wraps around the obstacle. We see that the helical pitch is shorter when the excitability ε^{-1} is increased.

An analysis of the dynamics of partially pinned scroll waves with different excitabilities ε^{-1} in the simulations is summarized in Fig. 7. The excitability (ε^{-1}) varies from 10 to 100 with a step of 10 and from 100 to 200 with a step of 20. When the excitability (ε^{-1}) is increased, the transient interval τ decreases [Fig. 7(a)] but the average speed s increases [Fig. 7(b)]. After the twist structures are completed, their helical pitch p is shorter [Fig. 7(c)], but with higher twist rate ω [Fig. 7(d)] in media with higher excitability ε^{-1} . In the graphs, a very small deviation of some points from the trend of the data set might be due to the large discretization of the space and time steps (0.2 s.u. and 0.012 t.u., respectively) used in this study. These simulation results are qualitatively similar to those in the experiments, Fig. 3. The

curves shown in Figs. 7(a)–7(d) can be well fit with the exponential functions: $\tau = 26.65 + 140.24\exp(-5.26 \times 10^{-2}\varepsilon^{-1})$ t.u., $s = 1.86 - 1.66\exp(-1.25 \times 10^{-2}\varepsilon^{-1})$ s.u. t.u. $^{-1}$, $p = 11.76 + 24.89\exp(-4.78 \times 10^{-2}\varepsilon^{-1})$ s.u., and $\omega = 32.89 - 22.86\exp(-1.93 \times 10^{-2}\varepsilon^{-1})^\circ$ s.u. $^{-1}$, respectively.

To confirm the common features found in the experiments (in Fig. 4), we consider the dynamics of simulated scroll

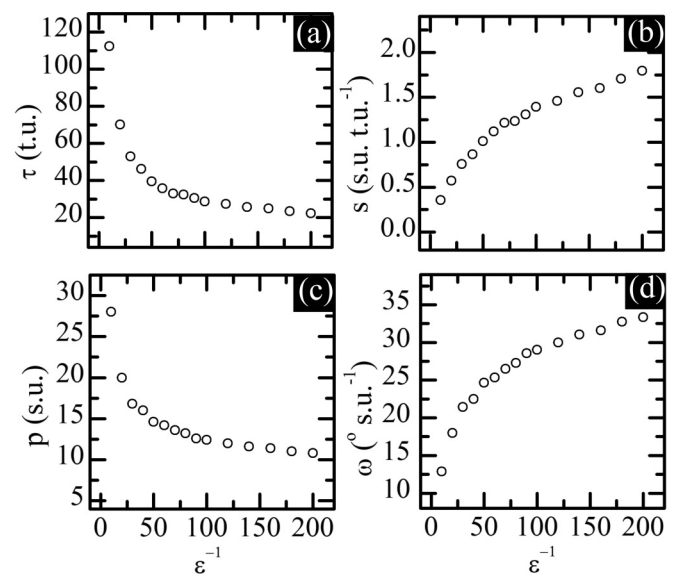


FIG. 7. Analysis of partially pinned scroll waves in the Oregonator model: (a) the transient time interval τ , (b) the average speed s , (c) the helical pitch p , and (d) the twist rate ω as functions of the parameter ε^{-1} .

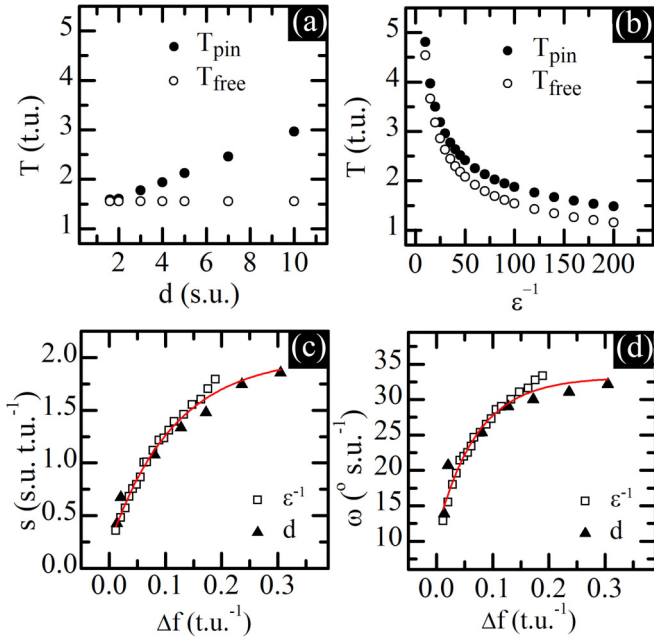


FIG. 8. Common features of partially pinned scroll waves in the Oregonator model. Periods of free and pinned parts at the beginning of the simulations with variations of (a) obstacle diameter d and (b) the parameter ϵ^{-1} . The average speed s (c) and the twist rate ω (d) of both simulation series, where the diameter d or the parameter ϵ^{-1} is varied, fit well to exponential functions of the difference in the initial frequency Δf .

waves in the current study and in [43]. Analysis of the simulations from [43] shows that when the obstacle diameter d is increased, the period of the pinned part T_{pin} decreases, but that of the free part T_{free} does not change [Fig. 8(a)]. In the current study, T_{pin} and T_{free} simultaneously decrease

with the parameter ϵ^{-1} [Fig. 8(b)]. These agree well with the experimental results in Figs. 4(a) and 4(b).

As shown in Fig. 8(c), we consider the average speed s of the downward motion of the twisted structure from the two studies with a variation of obstacle diameter d and the parameter ϵ^{-1} (triangles and squares, respectively). The average speed s fits well to an exponential function of the difference in the initial frequency Δf : $s = 2.00 - 1.79\exp(-8.76\Delta f)$ s.u. t.u.⁻¹. Similarly, Fig. 8(d) shows that the twist rate ω from both studies also fits with an exponential function: $\omega = 33.15 - 22.09 \exp(-14.04\Delta f)$ ° s.u.⁻¹. These two graphs confirm the common features in the experimental study in Figs. 4(c) and 4(d).

To simulate the development of partially pinned scroll waves in the presence of spontaneous waves as found in experiments (e.g., as in Fig. 5), we generate a scroll wave and many spherical waves at the beginning of a simulation, with $\epsilon^{-1} = 200$, as shown in Fig. 9. Three spherical waves are placed close to the core of the scroll wave to disturb the filament structure, while the others disrupt the outer wave fronts [Fig. 9(a)]. In the first few rotations, the disturbance of the scroll wave, especially in the lower pinned part of the scroll structure, almost disappears from the projection [Fig. 9(b)]. Then, the pinned twisted scroll wave is gradually developed downward on the obstacle while the disturbances are eliminated [Figs. 9(c) and 9(d)]. Finally, the entire medium is occupied solely by the partially pinned scroll wave [Fig. 9(e)], the same as without the spontaneous waves [Fig. 6(d)].

IV. DISCUSSION

We have determined the dynamics of scroll waves partially pinned to cylindrical obstacles in excitable media with a variation of excitability: The concentration sulfuric acid [H₂SO₄] in the BZ reaction and the parameter ϵ^{-1} in the Oregonator

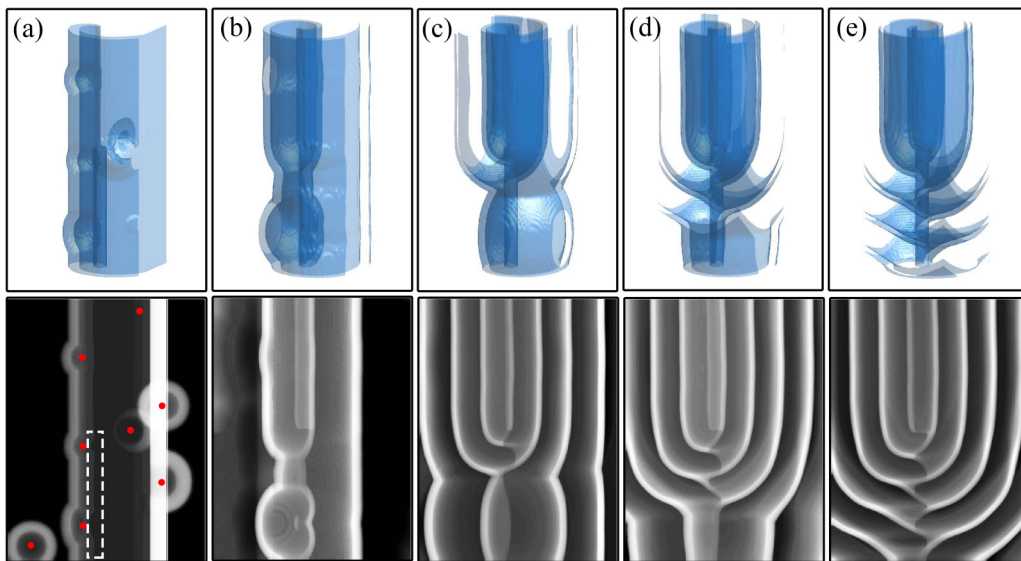


FIG. 9. Suppression of spontaneous waves by a partially pinned scroll wave in the Oregonator model with $\epsilon^{-1} = 200$ at times (a) 0.6, (b) 2.4, (c) 8.5, (d) 12.6, and (e) 21.5 t.u. The top and bottom rows depict isoconcentration surface plots of the inner volume and lateral projections of the volume, respectively. The white dashed rectangle and the red dots in (a) depict the cylindrical obstacle and the center of the spontaneous waves, respectively.

model are varied. Our experimental results agree well with numerical simulations. Initially, each scroll wave is straight, but the pinned region has a longer period than the freely rotating region. The interaction between the faster freely rotating wave and the obstacle results in a faster twisted wave that gradually displaces the slower untwisted pinned wave. Finally, the scroll wave helically wraps around the entire obstacle and the whole partially pinned scroll wave has the same period.

As the excitability of the medium is increased, both the average speed s of the twisted wave development and the twist rate ω increases. The earlier study [43] has shown similar increments of both the average speed s and the twist rate ω when the excitability was kept constant, but the obstacle diameter is enlarged. Thus the common features of these two studies are developed: Both the average speed s and the twist rate ω fit well to functions of the difference in the initial frequency Δf of the freely rotating and untwisted pinned waves.

In the BZ medium with high $[\text{H}_2\text{SO}_4]$, spontaneous waves may emerge during the scroll wave initiation. This study demonstrates the robustness of the partially pinned scroll waves against perturbations from such spontaneous waves. Even though the partially pinned scroll wave is partly disturbed, it gradually overcomes the other waves and the typical wave structure is developed as if in the absence of the spontaneous waves. Such suppression of spontaneous waves by wave pinning agrees well with the simulations using the

Fenton-Karma model [41,42] and the Barkley model [40] where the presence of thin cylindrical obstacles can both suppress and remove spatiotemporal patterns [40–42].

It has been shown earlier that without obstacles, twisted scroll waves in the BZ reaction can be induced by gradients in excitability, e.g., gradients in temperature [20,21], oxygen [22], or CO_2 concentration [23,24]. As in this study and in [43], the partial pinning to obstacles causes a step gradient in the wave period at the beginning and consequently the partially twisted scroll wave even in a medium with homogeneous excitability. In real situations, like cardiac media, both obstacles and gradients in excitability may present simultaneously and various occurrences of twisted scroll wave are anticipated. Such pinned scroll waves as presented in this study correspond to reentrant electrical waves pinned to heterogeneities, e.g., veins and scars, which cause longer-lasting tachycardia (i.e., high-frequency arrhythmia) in cardiac systems [25].

ACKNOWLEDGMENTS

We thank the Research and Development Institute (KURDI), Kasetsart University, the Thailand Research Fund (Grant No. RSA6280088), and the National Research Council of Thailand (Grant No. NRCT5-RGJ63002-029) for financial support. K.S. is grateful for support from the National Science Foundation (Grant No. CHE-2102137).

-
- [1] A. T. Winfree, *Science* **175**, 634 (1972).
 - [2] S. Nettesheim, A. von Oertzen, H. H. Rotermund, and G. Ertl, *J. Chem. Phys.* **98**, 9977 (1993).
 - [3] F. Siegert and C. J. Weijer, *J. Cell Sci.* **93**, 325 (1989).
 - [4] E. M. Cherry and F. H. Fenton, *New J. Phys.* **10**, 125016 (2008).
 - [5] S. C. Müller, T. Plesser, and B. Hess, *Science* **230**, 661 (1985).
 - [6] A. T. Winfree, *Science* **181**, 937 (1973).
 - [7] J. J. Tyson and S. H. Strogatz, *Int. J. Bifurcations Chaos* **1**, 723 (1991).
 - [8] A. T. Winfree, *Science* **266**, 1003 (1994).
 - [9] R. A. Gray, A. M. Pertsov, and J. Jalife, *Nature (London)* **392**, 75 (1998).
 - [10] F. Fenton, E. M. Cherry, H. M. Hastings, and S. J. Evans, *Chaos* **12**, 852 (2002).
 - [11] V. N. Biktashev, A. V. Holden, and H. Zhang, *Philos. Trans. R. Soc. A* **347**, 611 (1994).
 - [12] H. Henry and V. Hakim, *Phys. Rev. E* **65**, 046235 (2002).
 - [13] S. Alonso, F. Sagues, and A. S. Mikhailov, *Science* **299**, 1722 (2003).
 - [14] T. Bansagi and O. Steinbock, *Phys. Rev. E* **76**, 045202(R) (2007).
 - [15] C. Luengviriyai, U. Storb, G. Lindner, S. C. Müller, M. Bär, and M. J. B. Hauser, *Phys. Rev. Lett.* **100**, 148302 (2008).
 - [16] A. Rusakov, A. B. Medvinsky, and A. V. Panfilov, *Phys. Rev. E* **72**, 022902 (2005).
 - [17] D. Kupitz, S. Alonso, M. Bär, and M. J. B. Hauser, *Phys. Rev. E* **84**, 056210 (2011).
 - [18] C. Henze, E. Lugosi, and A. T. Winfree, *Can. J. Phys.* **68**, 683 (1990).
 - [19] I. Aranson and I. Mitkov, *Phys. Rev. E* **58**, 4556 (1998).
 - [20] A. M. Pertsov, R. R. Aliev, and V. I. Krinsky, *Nature (London)* **345**, 419 (1990).
 - [21] S. Mironov, M. Vinson, S. Mulvey, and A. M. Pertsov, *J. Phys. Chem.* **100**, 1975 (1996).
 - [22] U. Storb, C. R. Neto, M. Bär, and S. C. Müller, *Phys. Chem. Chem. Phys.* **5**, 2344 (2003).
 - [23] D. Kupitz and M. J. B. Hauser, *Phys. Rev. E* **86**, 066208 (2012).
 - [24] P. Dähmow, S. Alonso, M. Bär, and M. J. B. Hauser, *Phys. Rev. Lett.* **110**, 234102 (2013).
 - [25] J. M. Davidenko, A. M. Pertsov, R. Salomonz, W. Baxter, and J. Jalife, *Nature (London)* **355**, 349 (1992).
 - [26] J. P. Keener and J. J. Tyson, *Phys. D (Amsterdam)* **21**, 307 (1986).
 - [27] Y.-Q. Fu, H. Zhang, Z. Cao, B. Zheng, and G. Hu, *Phys. Rev. E* **72**, 046206 (2005).
 - [28] Z. Y. Lim, B. Maskara, F. Aguel, R. Emokpae, and L. Tung, *Circulation*, **114**, 2113 (2006).
 - [29] C. Cherubini, S. Filippi, and A. Gizzi, *Phys. Rev. E* **85**, 031915 (2012).
 - [30] M. Sutthiopad, J. Luengviriyai, P. Porjai, M. Phantu, J. Kanchanawarin, S. C. Müller, and C. Luengviriyai, *Phys. Rev. E* **91**, 052912 (2015).
 - [31] M. Tanaka, A. Isomura, M. Hörning, H. Kitahata, K. Agladze, and K. Yoshikawa, *Chaos* **19**, 043114 (2009).
 - [32] M. Tanaka, M. Hörning, H. Kitahata, and K. Yoshikawa, *Chaos* **25**, 103127 (2015).

- [33] M. Sutthiopad, J. Luengviriyaya, P. Porjai, B. Tomapatanaget, S. C. Müller, and C. Luengviriyaya, *Phys. Rev. E* **89**, 052902 (2014).
- [34] P. Porjai, M. Sutthiopad, J. Luengviriyaya, M. Phantu, S. C. Müller, and C. Luengviriyaya, *Chem. Phys. Lett.* **660**, 283 (2016).
- [35] Z. Jiménez, B. Marts, and O. Steinbock, *Phys. Rev. Lett.* **102**, 244101 (2009).
- [36] Z. Jiménez and O. Steinbock, *Europhys. Lett.* **91**, 50002 (2010).
- [37] Z. A. Jiménez and O. Steinbock, *Phys. Rev. E* **86**, 036205 (2012).
- [38] H. Ke, Z. Zhang, and O. Steinbock, *Phys. Rev. E* **91**, 032930 (2015).
- [39] S. Sridhar, A. Ghosh, and S. Sinha, *EPL* **103**, 50003 (2013).
- [40] F. Spreckelsen, D. Hornung, O. Steinbock, U. Parlitz, and S. Luther, *Phys. Rev. E* **92**, 042920 (2015).
- [41] Z. Zhang and O. Steinbock, *New J. Phys.* **18**, 053018 (2016).
- [42] Z. Zhang and O. Steinbock, *Chaos* **27**, 093921 (2017).
- [43] P. Porjai, M. Sutthiopad, K. Khaothong, M. Phantu, N. Kumchaiseemak, J. Luengviriyaya, K. Showalter, and C. Luengviriyaya, *Phys. Chem. Chem. Phys.* **21**, 2419 (2019).
- [44] R. J. Field and R. M. Noyes, *J. Chem. Phys.* **60**, 1877 (1974).
- [45] W. Jahnke and A. T. Winfree, *Int. J. Bifurcations Chaos* **1**, 445 (1991).
- [46] C. Luengviriyaya, U. Storb, M. J. B. Hauser, and S. C. Müller, *Phys. Chem. Chem. Phys.* **8**, 1425 (2006).
- [47] M. Dowle, R. M. Mantel, and D. Barkley, *Int. J. Bifurcations Chaos* **7**, 2529 (1997).
- [48] J. Luengviriyaya, M. Sutthiopad, M. Phantu, P. Porjai, J. Kanchanawarin, S. C. Müller, and C. Luengviriyaya, *Phys. Rev. E* **90**, 052919 (2014).